

Chapter 14

Application of Remote Sensing and Geographic Information System Techniques to Flood and Rainwater Harvesting: Case Study of Sennar, Sudan



Mohamad M. Yagoub and Sharaf Aldeen Mahmoud

Abstract Construction of the Grand Ethiopian Renaissance Dam will have positive and negative impacts on the people living downstream. Among possible impacts is the probability of flooding of human settlements along the Blue Nile. Reduction of water level is also a possible adverse effect of this dam on the agricultural schemes along the Blue Nile; the Gezira scheme, one of the largest irrigation projects in the world, could be affected by such reduction.

The objective of this study is twofold. The first objective is to identify cities and villages near the Sennar Dam (in Sudan) that may be affected by potential fluvial (river) floods. The location of the study area near the dam exposes it to a probable dam problem and, consequently, societal, environmental, and economic damages. Therefore, identifying vulnerable locations is crucial for reducing risk to lives and properties, for preparing contingency action plans, and for making the area more resilient. The second objective is to select rainwater-harvesting (RWH) sites that can be used for water-supply backup while minimizing possible water-level reduction. The use of remote-sensing and Geographic Information System (GIS) techniques in this study has enabled access to unique sources of information to better characterize hazards and risks.

Keywords Fluvial flood · Rainwater harvesting · Sennar Dam · Sudan · Remote sensing · GIS

M. M. Yagoub (✉) · S. A. Mahmoud

Department of Geography and Urban Sustainability, College of Humanities and Social Sciences, UAE University, Abu Dhabi, UAE

e-mail: myagoub@uaeu.ac.ae

14.1 Introduction

A large number of cities and villages in Sudan were impacted by fluvial floods during August–September 2020 (UNITAR, 2021). More than 80 people died and 380,000 were affected (FloodList, 2020). Water levels in the Blue Nile are higher than those in 1906 and close to the 1988 levels. This situation has created an urgent need for identifying potential areas that could be flooded in the future.

Global efforts that integrate remote sensing and a Geographic Information System (GIS) to create flood maps as preventive tools are increasing (Prinos, 2008; Wright, 2014). For example, in the U.S., the Federal Emergency Management Agency creates interactive maps for flood hazard or risk. Such maps support community resilience by providing data, building partnerships, and supporting long-term hazard-mitigation planning (FEMA, 2020). The UK Environment Agency (2020) provides real-time maps that show fluvial-flood risks. The Global Flood Awareness System (2020) of the European Commission Copernicus Emergency Management Service has an early-warning system that can be used to reduce flood impact. Other initiatives include the Global Flood Partnership, which provides a worldwide forum for exchange of experience about flood prediction, modeling, and flood risk (Global Flood Partnership, 2021). The United Nations Office for Disaster Risk Reduction (2021) plays a greater role in coordinating and following up with governments on implementation of the Sendai Framework. Accordingly, our study falls within the context of “Think globally, act locally.”

The study area includes the Sennar Dam, which is exposed to a probable flooding in case there is a problem at the Grand Ethiopian Renaissance Dam (GERD). Previous studies around the world have showed the potential risk of dam failure due to natural disasters or inadequate maintenance and management (Butt et al., 2013; Cenderelli, 2000; de Paiva et al., 2020; FEMA, 2013; Finn, 2008; Harrigan et al., 2020). Types of dam failure include dam body instability, canal gushing and soil flow, dam cracking, dam overtopping, and pilot-system failure (Escuder-Bueno et al., 2016; Kuo et al., 2007; Michailidi & Bacchi, 2017; Micovic et al., 2016; Yang et al., 2020). Discharge from a dam is governed by the maximum reservoir water level, reservoir capacity, and maximum discharge capacity. The seasonal variation in Blue Nile discharge ranges from 60 m³/s in a very low year to >10,000 m³/s at the peak of a high flood (Plusquellec, 1990).

Floodwater can be used to enable communities to make smart water-management decisions even during times of relative water abundance. Flooding can help resurrect wetlands and slow down climate change. Rainwater harvesting (RWH) includes gathering and storing rainwater to be used for drinking, irrigation, and livestock (Abdulrazzak, 2003; Awawdeh et al., 2012; Critchley et al., 1991; Galarza-Molina et al., 2015; Gould and Nissen-Petersen, 1999; Jha et al., 2014; Singh et al., 2016; Tiwari et al., 2018). RWH can also improve sustainability and reduce the impact of climate change (African Development Bank, 2010; UNEP, 2009). RWH has been

gaining momentum worldwide. For example, Inamdar et al. (2013) used GIS to determine suitable locations for stormwater collection in Melbourne, Australia. They used runoff, open space, and accumulated catchments as criteria. They concluded that Royal Park ranked high for RWH as it had the largest water demand and the drainage outlets were close to the site.

Elhag and Bahrawi (2014) performed a study in the Kingdom of Saudi Arabia to improve RWH in terms of groundwater recharge. They created a spatiotemporal cloud map for evaluating prior-delineated watersheds that are beneath mostly cloudy skies all year. They used satellite imagery (EnviSat and Landsat), a digital elevation model (DEM), and soil-moisture and geological data. Singhai et al. (2017) used a combination of satellite images, land-use and soil data, and multi-criteria decision analysis to identify natural depression sites for RWH and found that forested areas have low-runoff potential whereas built-up areas have high-runoff potential.

Once potential RWH sites are identified, a suitable method can be employed to store water. Among the methods used are bound or terrace practices in areas with low-infiltration soil, small dams, micro-catchments, and haffirs. A haffir is an artificial excavation into which surface-water runoff is diverted during the rainy season. Its size depends on the location, hydrology, soils, and rainfall (Salih et al., 2016).

14.2 Study Area

The area around Sennar city was selected because of the availability of data, location of Sennar Dam (~260 km south of Khartoum), and the importance of the dam to the Sudanese economy (Gezira irrigation scheme).

The area includes Sennar and many other villages. Historically, the city of Sennar has been known as a major hub since the era of the Funj Chronicle (1504–1821). The city is at lat 13.539510 N and long 33.611298 E and is within UTM Zone 36 N, with an average altitude of 434.87 m (Fig. 14.1). The area includes schools, a university, hospitals, administration offices, and many banks. Most of its population (~1.5 million) depend on trade, agriculture, livestock, and services.

The average temperature in winter is 25 °C; in summer, it is 40 °C. The rainy or wet season in the study area starts in May and ends in October.

Flooding in the Blue Nile commences in May and reaches its climax during middle to late August–September. The average monthly rainfall (based on the period 2016–2019) ranges within 20–100 mm and reaches its maximum during August.

Built on the Blue Nile, the Sennar Dam was completed in 1925. Its main objective is to supply water for the Gezira irrigation scheme (Bernal, 1997). Its total storage capacity is 930 million cubic meter (Roseires Dam reservoir holds 3 billion cubic meter). The Sennar Dam is 3025-m long with a maximum height of 40 m. Two

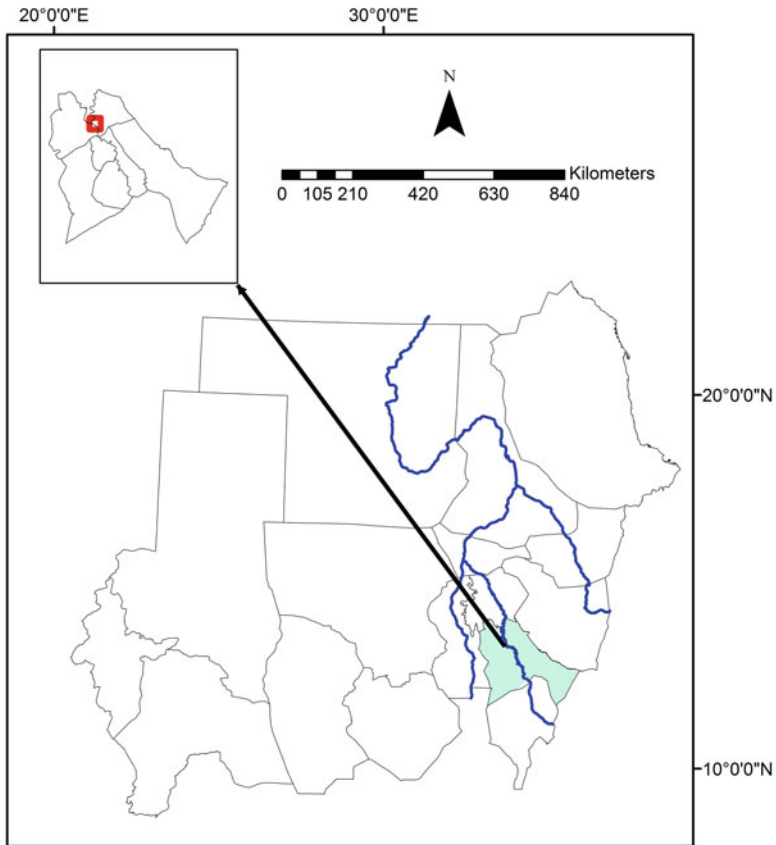


Fig. 14.1 Location of the study area

canals with numerous branches (4300 km) are used to irrigate the Gezira and Managil schemes. The minimum level in the reservoir to maintain maximum flow in the Gezira canal is 417.2 m while the top water level of the reservoir is 421.7 m (Plusquellec, 1990). A road and a rail route run along the length of the dam (The Engineer, 1924).

GERD is physically not within the study area, but its impact is the main objective of this study. The GERD has a planned full supply elevation of 640 m, 74 billion cubic meter of reservoir storage, and 6000 megawatt of installed generation capacity (Wheeler et al., 2016). The benefits of GRED could be in reduction of the flooding risk to Sudan, reduction of sediment in the river, reliability of flows, hydropower benefits, improved depth for navigation and reduced pumping costs for water users (Wheeler et al., 2016). However, on the other side GERD may reduce downstream water availability, impact on agriculture in Sudan, reduce land fertility due to the reduction of nutrient-rich sediment, and possible environmental impacts (Beyene, 2013).

14.3 Data

Data collected to identify settlements at risk and suitable RWH locations are shown in Table 14.1.

14.4 Methodology

The methodology for identifying potential areas that can be impacted by fluvial floods was based on land-use and elevation data, the topographic wetness index (TWI), and proximity to Blue Nile (1–3 km). Five experts were consulted for setting the weight for each factor. Based on their recommendations resulting from their use of the Analytical Hierarchy Process (Saaty, 1980; Teknomo, 2020). Land use, elevation, TWI, and proximity to Blue Nile were assigned the weights of 0.2, 0.2, 0.3, and 0.3, respectively. All data were saved in raster format, and ArcGIS software was used in the subsequent analysis. Values in each layer were coded to a common scale of 1 (very low risk) to 5 (very high risk), and a weighted overlay was generated for all the layers. The result was classified into high, medium, and low-risk zones, and the number of people in each zone was calculated.

Land-use map generated using the Sentinel-2 satellite image of May 22, 2020 was one of the inputs. Sentinel-2 satellite data has a better resolution (10 m for Bands 2, 3, 4, and 8) than Landsat 8 (30 m). The month of May was selected because it is summertime and hence less cloudy. Bands 2 (blue), 3 (green), and 4 (red) were merged to generate a composite image. The ISO cluster unsupervised classification method was used to create a signature file, which is used to aid supervised classification. Training sites for barren (30 samples), built-up (40 samples), farms (30 samples), gardens and orchards (30 samples), and water (30 samples) were digitized using the ArcGIS software. A higher number of training samples was taken for built-up areas in case of the mixture of buildings with trees. The maximum-likelihood

Table 14.1 Data collected to identify settlements at risk and suitable rainwater-harvesting sites

	Data	Source	Format
1.	30-m-resolution digital elevation model (DEM)	U.S. Geological Survey Earth Explorer https://earthexplorer.usgs.gov/	Raster
2.	Sentinel-2 Tile Number: T36PWA Date: May 22, 2020	Copernicus Open Access Hub https://scihub.copernicus.eu/	Raster
3.	Land use	Sentinel-2 satellite image	Vector
4.	Population	Sennar Municipality	Vector
5.	2-m-resolution DEM from aerial photos obtained in 2010	Sennar Municipality	Raster
6.	Monthly rainfall data (2009–2018)	World Weather Online https://www.worldweatheronline.com/	Text

classifier algorithm was used for supervised classification. To check the accuracy of classification, 500 points were used. A majority filter (eight neighbors) was used to smoothen class boundaries and remove small isolated regions. The Boundary Clean was used to increase the spatial coherency of the classified image and connect adjacent regions (ESRI, 2017). Small isolated regions on the classified image were removed by applying the region/group method, which is a generalization process.

The normalized difference vegetation index (NDVI) (Richards, 2013) was calculated from Sentinel-2 data using band 4 as the red band (10-m resolution) and Band 8a as the infrared band (20-m resolution) (ESA, 2020):

$$\text{NDVI} = (\text{Infrared band} - \text{Red band}) / (\text{Infrared band} + \text{Red band}) \quad (14.1)$$

NDVI was used to identify water comprising the Blue Nile. NDVI values were found to be between -1.0 and 1.0 . Negative values represent clouds and water, while high positive values (0.6 – 0.8) indicate temperate and tropical rainforests. Raster calculator was used to identify areas with NDVI values close to 0 or negative (Blue Nile water).

30-m-resolution DEM was used initially to obtain a quick overview of the topography of the area. Sinks and peaks within the DEM were removed using the fill tool. The methodology for identifying potential RWH sites was based on creating morphometric variables from the high-resolution (2-m) DEM derived from aerial photographs (Table 14.1). The variables included surface slope, flow direction, flow accumulation, and TWI. TWI provides information about flood and surface ponding at a reasonable cost compared to hydrologic and hydraulic modeling (Ballerine, 2017; Beven et al., 1979; Buchanan et al., 2014; Dilts, 2015; Qin et al., 2011; Wolock and McCabe, 1995; Yagoub et al., 2020). TWI was generated in ArcGIS software (using the D8 algorithm to model flow into a single downslope cell). TWI results were passed through a filtering, smoothing, and generalization process similar to that used for land-use classification. The large sites identified from TWI were manually digitized for calculation of areas, addition of other attributes, and cartographic output. The sites were further assessed for determining the land-use type (and whether a site is a vacant land), proximity to Blue Nile, and total area.

14.5 Results

Water (Blue Nile) and soil could not be distinguished in the supervised classification of the Sentinel-2 satellite image from May 22, 2020 as they have similar spectral characteristics. The confusion resulted from the brown color of the sediment-laden river. Generally, every year, rain starts in Ethiopia during April–May and continues in Sudan until September–October. This indicates that it is difficult to classify Blue Nile water for almost 6 months during most years. To address this problem, NDVI data were derived and water was identified as having negative NDVI values. Then, the water was used as training samples. This method achieved better results than

taking training samples from water without the use of NDVI. The NDVI values for the May 22, 2020 image ranged between -0.49 and 0.79 .

Table 14.2 shows the confusion-error matrix. Classification accuracy of the land-use map is 95.6% and Kappa statistic is 0.92; the classification accuracy meets the recommended accuracy of $\geq 85\%$ suggested by Foody (2002). A large portion of the area (77%) is classified as farmland and fallow fields (Table 14.3); this includes agricultural schemes in Eastern Sennar and part of Gezira. Built-up areas were assigned a high flood-potential value (scale of 5) while barren areas were given low values (Table 14.3).

Elevation is an important parameter in describing floodwater. The elevation in the area ranges within 405–436 m above mean sea level (Fig. 14.2; Table 14.4). Low and very low areas comprise 10% of the area (Table 14.4). The Blue Nile was masked, and its elevation was found to range within 405–428 m (Fig. 14.2). Because this shows reservoir-water-level height downstream and upstream from the dam, the difference in height can be used for calculating the storage volume of the dam (Butt et al., 2013). The obtained value of 428 m may represent islands inside the reservoir, given that the water level of the reservoir is kept at 421.7 m.

There are 11 villages and seven districts within Sennar city (population: 32,950) that fall within the high flood-potential zone (Table 14.5; Figs. 14.3 and 14.4), which includes 37 mosques, 36 schools, eight clinics, and one church. This indicates that a large number of people and infrastructure may be impacted by potential fluvial

Table 14.2 Confusion matrix

Class	Barren	Built-up	Farms	Gardens and orchards	Water	Total	User's accuracy
Barren	58	9	1			68	0.852
Built-up		38				38	1.0
Farms	2	3	326			331	0.984
Gardens and orchards	4			28	1	33	0.848
Water	2				29	31	0.935
Totals	66	50	327	28	30	501	0.0
Producer's accuracy	0.8787	0.7600	0.9969	1	0.9666	0.0	0.956
Kappa	0.92						

Table 14.3 Land use as of May 22, 2020

Class	Scale	Area (km ²)	Percentage
Barren	2	34	10
Built-up	5	23	6
Farmland and fallow fields	3	271	77
Gardens	4	26	7
Total		354	100

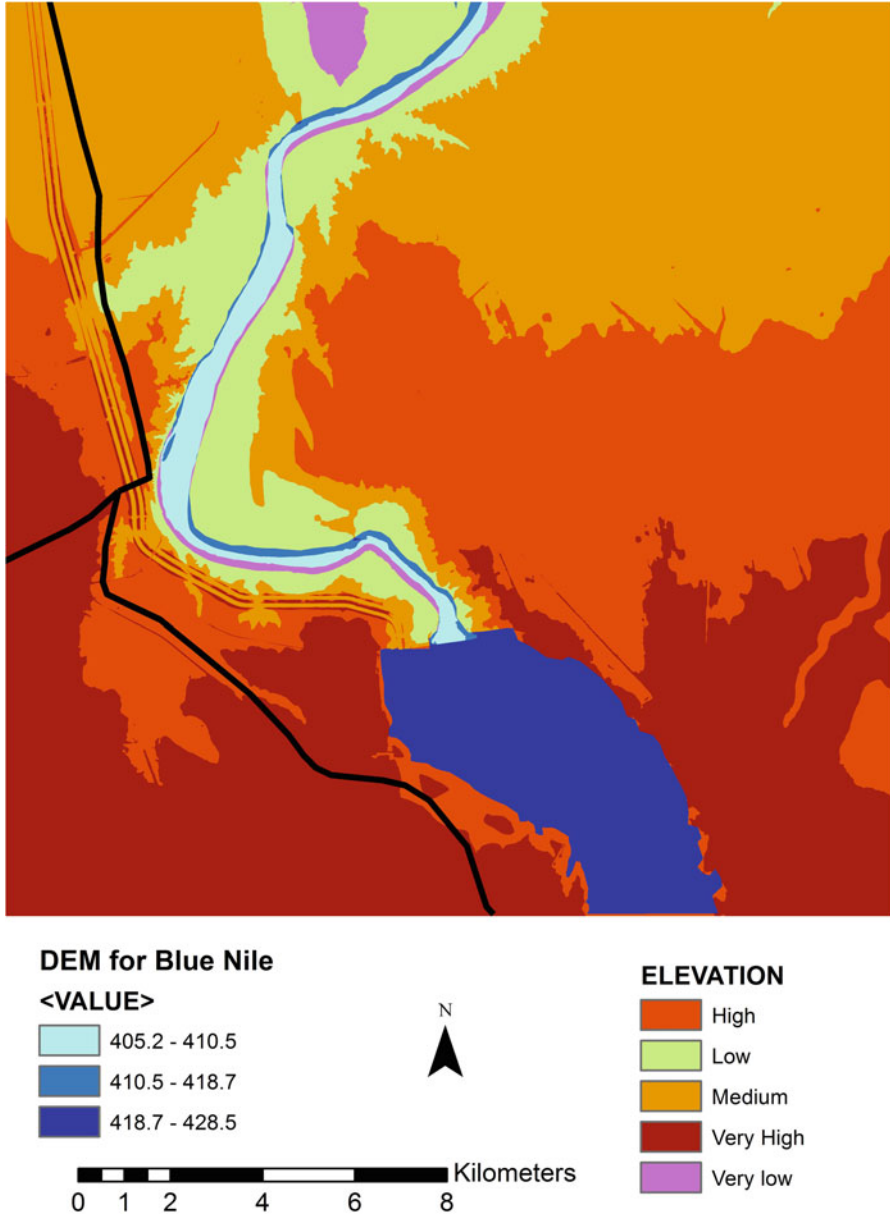


Fig. 14.2 Elevation categories

flooding. The area around Sennar Dam can get flooded if the water at the dam exceeds the flood level and the inflow is more than the discharge capacity. Furthermore, possible dam failure would affect the Gezira irrigation scheme, which supplies water to an area of over 882,000 ha where many farmers grow crops (cotton, wheat,

Table 14.4 Elevation classes

Value (m)	Scale	Area (km ²)	Percentage	Elevation class
405.1–411.3	5	4	1	Very low
411.3–418.4	4	33	9	Low
418.4–423.0	3	113	32	Medium
423.0–425.9	2	104	29	High
425.9–436.1	1	100	28	Very high
Total		354	100	

Table 14.5 Areas at potential fluvial flood zone

	Village/district name	Flood potential level	Population potentially exposed to flood
1.	Al Tikina	High ^a	682
2.	Al Islahia	High ^a	135
3.	Al Jinina	High ^a	3432
4.	Karima Abdel Rasoul	High	1483
5.	Karima Bahar	High	2168
6.	Al Arakeen	High	2318
7.	Banat	High	305
8.	Neel District (Sennar city)	High	3228
9.	Gala East District (Sennar city)	High	4418
10.	Taktok District (Sennar city)	High	1804
11.	Morba 22 and 23 district (Sennar city)	High	2749
12.	Soug District (Sennar city)	High	156
13.	Morba 21 South District (Sennar city)	High	1458
14.	Morba 21 North District (Sennar city)	High	1769
15.	Sharif Bajboj	High	1747
16.	Kasab Grabi	High	2282
17.	Kasab Jaleen	High	1545
18.	Kasab Danagla	High	1271
			32,950

^aAreas at higher risk because they are downstream from and close to the dam

groundnuts, and sorghum) and on which traders and livestock depend (Bernal, 1997; Gaitskell, 1959). Therefore, there is an urgent need for backup plans and scenarios on how to deal with reduction of water level, flood spill from GERD, or dam failure, taking into account that the Blue Nile contributes ~57% of the yield of the Nile (Wheeler et al., 2016). Insufficient water supply in the past (1984–1985) resulted in the cessation of wheat cultivation in the area (Plusquellec, 1990).

Contributing ~35% of the Gross National Product, the Gezira scheme has been the backbone of the Sudanese economy for many years.

TWI values in the area range between 1 and 25 (Table 14.6; Fig. 14.5), whereas in a study conducted in the U.S. (Illinois), TWI indicators were found to range between –3 and 30 although they varied according to topography (Ballerine, 2017). Higher

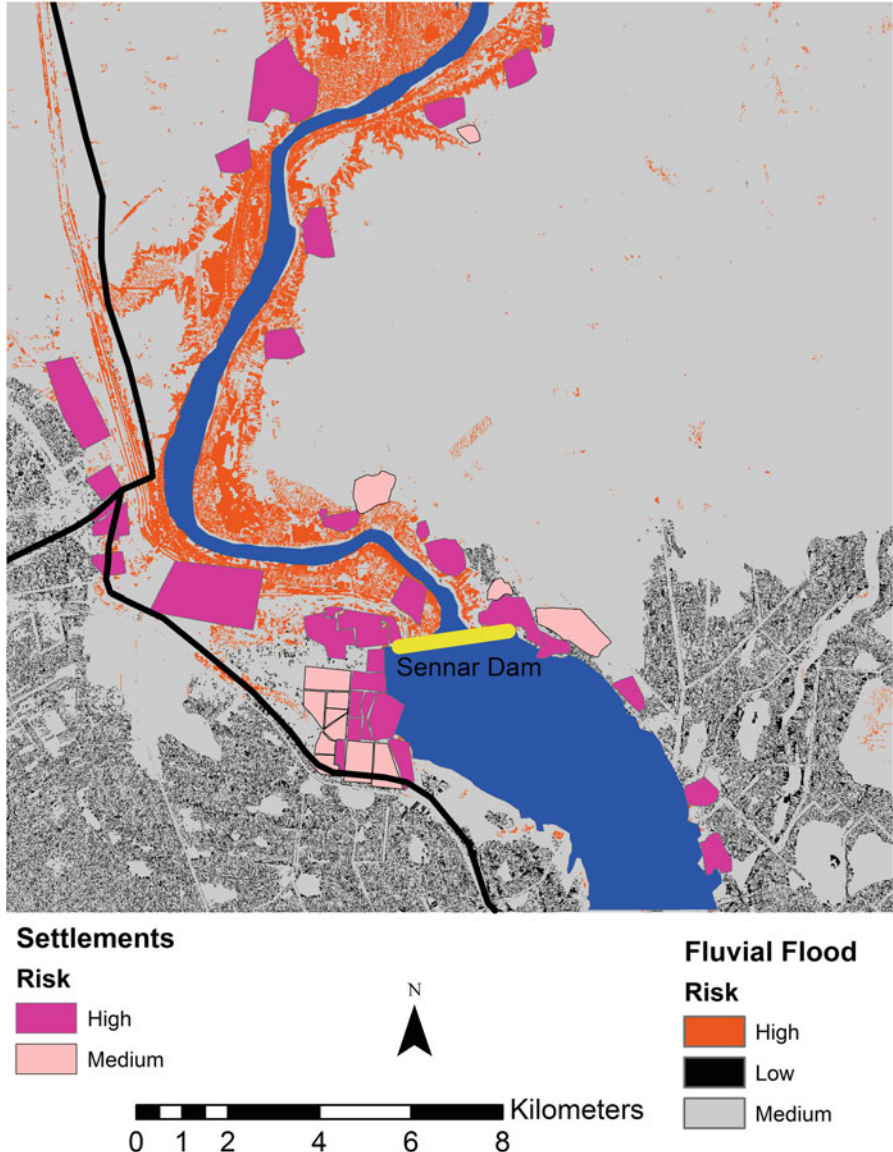


Fig. 14.3 Areas in potential fluvial-flood zone

TWI values occur where greater upslope areas drain into a gentle local slope, and lower values indicate less potential for ponding (Wolock & McCabe, 1995). Based on TWI values, the threshold value for TWI to be classified as potential RWH sites was set to 12. This threshold value is set manually with the aid of symbolization and may vary from one region to another depending on topography. Thus, TWI values of

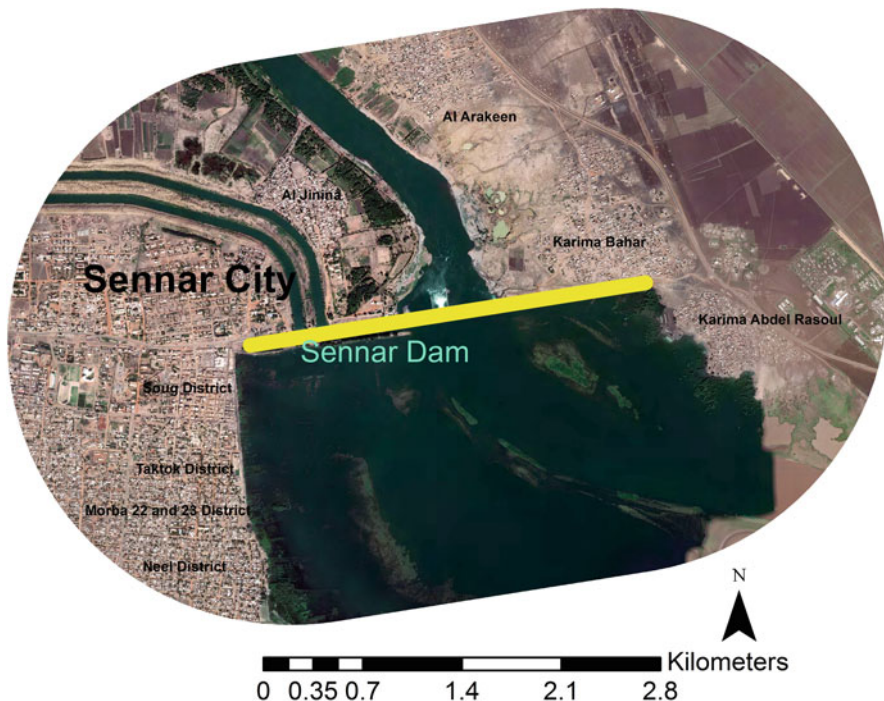
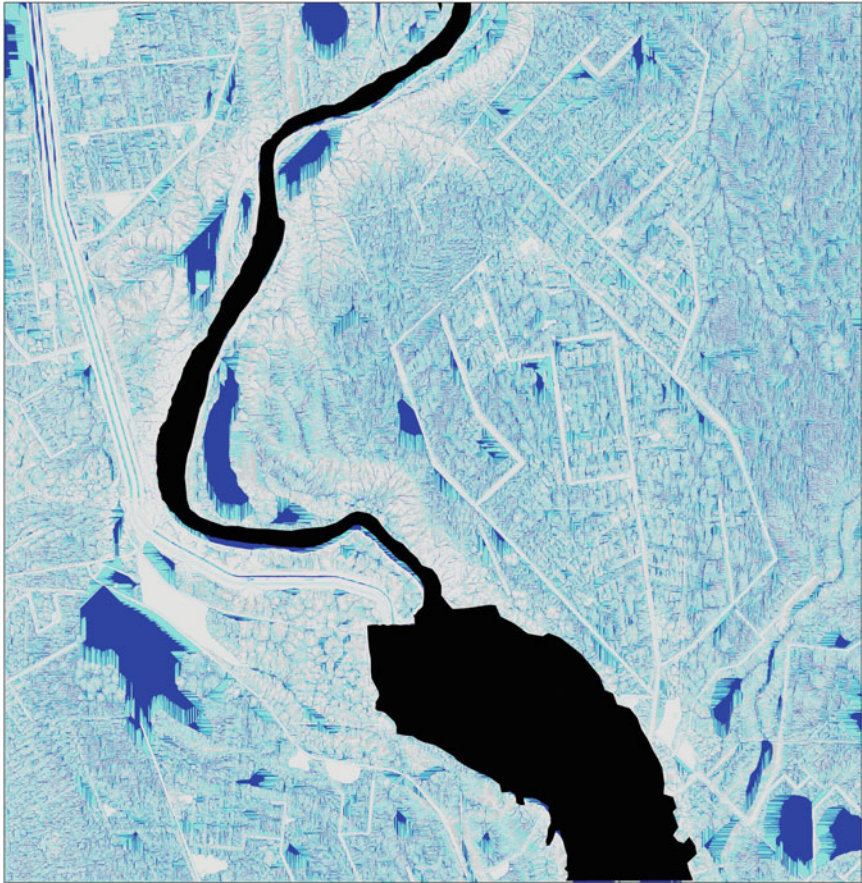


Fig. 14.4 Settlements within 2 km of Sennar Dam

Table 14.6 Topographic wetness index values

Value	Scale	Area (km ²)	Percentage
1–7	1	122	34
7–9	2	99	28
9–12	3	75	21
12–15	4	49	14
15–25	5	9	3
	Totals	354	100

>12 are assigned high scale values (Table 14.6; Fig. 14.5). Seven potential RWH sites were identified using TWI as the main criterion (Fig. 14.6). Sites 1–4 are close to the Blue Nile and can be conserved as ponds, wetland, or floodplain areas to divert water in case of fluvial flooding. Site 6 (Table 14.7; Fig. 14.6) has the largest area, but it is not suitable for RWH because it is surrounded by built-up areas, and the site can be used for future expansion of the city. Sites 5 and 7 are best for RWH and should be further assessed in terms of soil and ownership. The haffir method is proposed for potential RWH sites because it is less expensive. In addition, trees can be planted around such RWH sites. Check dams, which are small dams constructed across a valley or channel to lower the velocity of flow and to recharge groundwater, are also recommended to be constructed in valleys or khors. (Sandbags filled with pea gravel and logs can be used.)




Legend

 Blue Nile

TWI

<VALUE>

 0.837397158 - 7.873770729

 7.87377073 - 10.12150117

 10.12150118 - 12.76014126

 12.76014127 - 25.75788689

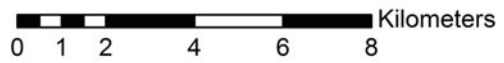


Fig. 14.5 Topographic wetness index values

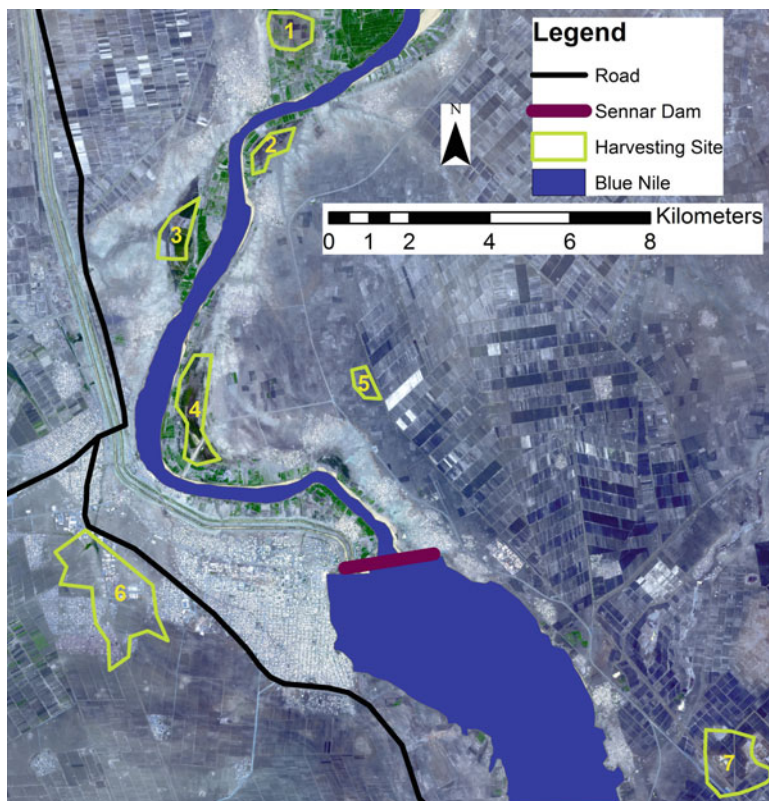


Fig. 14.6 Possible rainwater-harvesting sites

Table 14.7 Possible rainwater-harvesting sites

Site number	Area (km ²)	Percentage	Distance from Blue Nile (km)	Potential use
1	0.8646	8.39	1–2	Floodplain areas
2	0.5521	5.36	1	Floodplain areas
3	0.8676	8.42	1	Floodplain areas
4	1.6019	15.54	1	Floodplain areas
5	0.3306	3.21	2–3	Rainwater harvesting
6	4.1412	40.17	2–3	Excluded
7	1.9520	18.93	2–3	Rainwater harvesting
Total	10.3101	100		

14.6 Conclusion

In this study, settlements at a potential fluvial flood around Sennar Dam in Sudan were identified. The obtained results require further evaluation but can be used as a general guide for a sudden dam breach, insurance, impact assessment, emergency management, and developing effective flood plans. Seven possible RWH sites were also delineated. These sites will increase the coping capacity of the population with respect to shocks produced from rainfall variation and reduction of water flow due to GERD construction. The sites can be used for agriculture, livestock, and other purposes, and they will have a positive socioeconomic impact on the livelihoods of the inhabitants. The accuracy of the obtained results is affected by the population count and the accuracy of the land-use classification and DEM. TWI results depend on the DEM cell size, slope algorithm, flow-direction algorithm, and errors during either the acquisition or processing of aerial photographs.

The main causes of fluvial floods in Sudan during August–September, 2020 were high water level and building construction along the banks of the rivers. The buildings near the banks narrowed the rivers' width and altered their natural flow. Therefore, urban planning needs to take this into account, and collaboration and coordination among various stakeholders is needed (dam managers, urban planners, civil-defense officers, climate specialists, etc.). Furthermore, public awareness about flood hazards is very important. Future study could include using hydraulic and hydrological models to generate water-surface profiles for a given flood event (such as a 50-year flood), to determine the height of water across the river at a given location, to characterize the propagation of flood waves, and to map effects in the valley downstream from the dam structure. Similar studies can be conducted concerning the multipurpose Roseires Dam.

Acknowledgments The authors are grateful to UAE University Research Affair.

Office for support. The authors are also indebted to Prof. Mashael M. Al Saud (Space Research Institute, King Abdel Aziz City for Science and Technology) for her encouragement and support to participate in a book entitled "Applications of Remote Sensing on the Natural Hazards in the MENA Region". Mr. Shehab Majud is acknowledged for his following up with the editing process.

References

- Abdulrazzak, M. (2003). *Water harvesting practices in selected countries of the Arabian Peninsula*. Conference on water harvesting and the future development, Khartoum, Sudan, 19–20 August 2003.
- African Development Bank. (2010). *Assessment of best practices and experience in water harvesting: Rainwater harvesting handbook* (75 pp.). ADB, Cote d'Ivoire, Open File Rep.
- Awawdeh, M., Al-Shraideh, S., Al-Qudah, K., & Jaradat, R. A. (2012). Rainwater harvesting assessment for a small size urban area in Jordan. *International Journal of Water Resources and Environmental Engineering*, 4, 415–422.

- Ballerine, C. (2017). *Topographic Wetness Index, Urban Flooding Awareness Act, action support: Will and DuPage Counties, Illinois*. Contract report 2017-02, April 2017, Illinois state. <https://www.ideals.illinois.edu/handle/2142/98495>. Accessed 5 Jan 2021.
- Bernal, V. (1997). Colonial moral economy and the discipline of development: The Gezira Scheme and “Modern” Sudan. *Cultural Anthropology*, 12(4), 447–479. <https://doi.org/10.1525/can.1997.12.4.447>
- Beven, K. J., Kirkby, M. J., & Seibert, J. (1979). A physically based, variable contributing area model of basin hydrology. *Hydrological Sciences Bulletin*, 24, 43–69.
- Beyene, A. (2013). *Reflections on the Grand Ethiopian Renaissance Dam*. <http://www.opride.com/oromsis/news/horn-of-africa/3664-reflections-on-the-grandethiopian-renaissance-dam>. Accessed 18 Jan 2021.
- Buchanan, B. P., Fleming, M., Schneider, R. L., Richards, B. K., Archibald, J., Qiu, Z., & Walter, M. T. (2014). Evaluating topographic wetness indices across Central New York agricultural landscapes. *Hydrology and Earth System Sciences*, 18(8), 3279–3299. <http://www.hydrol-earth-syst-sci.net/18/3279/2014/hess-18-3279-2014.pdf>. Accessed 8 Jan 2021.
- Butt, M. J., Umar, M., & Qamar, R. (2013). Landslide dam and subsequent dam-break flood estimation using HEC-RAS model in northern Pakistan. *Natural Hazards*, 65, 241–254. <https://doi.org/10.1007/s11069-012-0361-8>
- Cenderelli, D. A. (2000). Floods from natural and artificial dam failures. In E. E. Wohl (Ed.), *Inland flood hazards* (pp. 73–103). Cambridge University Press.
- Critchley, W., Siegert, K., Chapman, C., & Finkel, M. (1991). *Water harvesting: A manual for the design and construction of water harvesting schemes for plant production* (154 pp.). Food and Agriculture Organization of the United Nations, Open File Rep.
- de Paiva, C. A., da Fonseca, S. A., & do Prado, F. J. F. (2020). Content analysis of dam break studies for tailings dams with high damage potential in the Quadrilátero Ferrífero, Minas Gerais: Technical weaknesses and proposals for improvements. *Natural Hazards*, 104, 1141–1156. <https://doi.org/10.1007/s11069-020-04254-8>
- Dilts, T. E. (2015). *Topography tools for ArcGIS 10.1*. University of Nevada Reno. <https://www.arcgis.com/home/item.html?id=b13b3b40fa3c43d4a23a1a09c5fe96b9>. Accessed 4 Jan 2021.
- Elhag, M., & Bahrawi, J. A. (2014). Conservational use of remote sensing techniques for a novel rainwater harvesting in arid environment. *Environment and Earth Science*, 72, 4995–5005.
- Environmental Systems Research Institute (ESRI). (2017). ArcGIS Desktop 10.5.1. ESRI Incorporation.
- Escuder-Bueno, I., Mazza, G., Morales-Torres, A., & Castillo-Rodriguez, J. T. (2016). Computational aspects of dam risk analysis: findings and challenges. *Engineering*, 2(3), 319–324.
- European Space Agency (ESA). (2020). *The spatial resolution of SENTINEL-2*. <https://sentinel.esa.int/web/sentinel/user-guides/sentinel-2-msi/resolutions/spatial>. Accessed 15 Jan 2021.
- Federal Emergency Management Agency (FEMA). (2013). *Federal guidelines for dam safety emergency action planning for dams*. <https://www.fema.gov>. Accessed 7 Jan 2021.
- Federal Emergency Management Agency (FEMA). (2020) *Risk mapping, assessment and planning (Risk MAP)*. <https://www.fema.gov/flood-maps/tools-resources/risk-map>. Accessed 7 Jan 2021.
- Finn, H. (2008). *Dam failure and inundation modeling: Test case for ham dam*. Summary report, project conducted by “DHI Gulf” for UAE Ministry of Environment & Water.
- FloodList. (2020). *Sudan – Over 80 dead and 380,000 affected as floods worsen*. <https://floodlist.com/africa/sudan-khartoum-floods-august-2020>. Accessed 2 Sept 2020.
- Foody, G. M. (2002). Status of land cover classification accuracy assessment. *Remote Sensing of Environment*, 80(2002), 185–201.
- Gaitskell, A. (1959). *Gezira: a story of development in the Sudan*. Faber and Faber.
- Galarza-Molina, S., Torres, A., Moura, P., & Lara-Borrero, J. (2015). CRIDE: A case study in multi-criteria analysis for decision making support in rainwater harvesting. *International Journal of Information Technology & Decision Making*, 14, 43–67. <https://doi.org/10.1142/S0219622014500862>
- Global Flood Awareness System (GloFAS). (2020). www.globalfloods.eu. Accessed 7 Jan 2021.

- Global Flood Partnership. (2021). <https://gfp.jrc.ec.europa.eu/>. Accessed 18 Jan 2021.
- Gould, J., & Nissen-Petersen, E. (1999). *Rainwater catchment systems for domestic supply: Design, construction and implementation*. Intermediate Technology Publications.
- Harrigan, S., Zsoter, E., Alfieri, L., Prudhomme, C., Salamon, P., Wetterhall, F., Barnard, C., Cloke, H., & Pappenberger, F. (2020). GloFAS-ERA5 operational global river discharge reanalysis 1979–present. *Earth System Science Data Discussions*. <https://doi.org/10.5194/essd-2019-232>
- Inamdar, P. M., Cook, S., Sharma, A. K., Corby, N., O'Connor, J., & Perera, B. J. (2013). A GIS based screening tool for locating and ranking of suitable stormwater harvesting sites in urban areas. *Journal of Environmental Management*, 128, 363–370.
- Jha, M., Chowdary, V., Kulkarni, Y., & Mal, B. (2014). Rainwater harvesting planning using geospatial techniques and multicriteria decision analysis. *Resources, Conservation and Recycling*, 83, 96–111. <https://doi.org/10.1016/j.resconrec.2013.12.003>
- Kuo, J. T., Yen, B. C., Hsu, Y. C., et al. (2007). Risk analysis for dam overtopping—Feitsui reservoir as a case study. *Journal of Hydraulic Engineering*, 133(8), 955–963.
- Michailidi, E. M., & Bacchi, B. (2017). Dealing with uncertainty in the probability of overtopping of a flood mitigation dam. *Hydrology and Earth System Sciences*, 21(5), 2497–2507.
- Micovic, Z., Hartford, D. N. D., Schaefer, M. G., & Barker, B. L. (2016). A non-traditional approach to the analysis of flood hazard for dams. *Stochastic Environmental Research and Risk Assessment*, 30(2), 559–581.
- Plusquellec, H. (1990). *The Gezira irrigation scheme in Sudan: Objectives, design, and performance*. World Bank Technical Paper Number 120. The World Bank.
- Prinos, P. (2008). *Review of flood hazard mapping*. European Community sixth framework programme for European Research and Technological Development. FLOODsite. www.floodsite.net. Accessed 14 Dec 2020.
- Qin, C. Z., Zhu, A. X., Pei, T., Li, B.-L., Scholten, T., Behrens, T., & Zhou, C.-H. (2011). An approach to computing topographic wetness index based on maximum downslope gradient. *Precision Agriculture*, 12(1), 32–43. <https://doi.org/10.1007/s11119-009-9152-y>
- Richards, J. A. (2013). *Remote sensing digital image analysis: an introduction*. Springer. <https://www.springer.com/gp/book/9783642300615>. isbn 978-3-642-30062-2
- Saaty, T. L. (1980). *The analytic hierarchy process*. McGraw Hill.
- Salih, A., Ahmed, A. S., & Yousif, T. A. (2016). *Water harvesting practices and techniques in Sudan from perspective of remote sensing and GIS*. Water harvesting symposium, University of Khartoum, Khartoum, Sudan.
- Singh, L., Jha, M., & Chowdary, V. (2016). Multi-criteria analysis and GIS modelling for identifying prospective water harvesting and artificial recharge sites for sustainable water supply. *Journal of Cleaner Production*, 142, 1436–1456. <https://doi.org/10.1016/j.jclepro.2016.11.163>
- Singhai, A., Das, S., Kadam, A. K., Shukla, J. P., Bundela, D. S., & Kalashetty, M. (2017). GIS-based multi-criteria approach for identification of rainwater harvesting zones in upper Betwa sub-basin of Madhya Pradesh, India. *Environment, Development and Sustainability*, 21, 777–797. <https://doi.org/10.1007/s10668-017-0060-4>
- Teknomo, K. (2020). *Analytic hierarchy process (AHP) tutorial*. Available online: <https://people.revoledu.com/kardi/tutorial/>. Accessed 7 Jan 2021.
- The Engineer. (1924, September 26). The Sennar Dam and Gezira Irrigation Scheme. *The Engineer*, pp. 349–50. <https://www.gracesguide.co.uk/Special:Search?search=Sennar+dam&fulltext>. Accessed 4 Jan 2021.
- Tiwari, K., Goyal, R., & Sarkar, A. (2018). GIS-based methodology for identification of suitable locations for rainwater harvesting structures. *Water Resources Management*, 32, 1811–1825. <https://doi.org/10.1007/s11269-018-1905-9>
- UK Environment Agency. (2020). *Check your long-term flood risk*. <https://flood-warning-information.service.gov.uk/long-term-flood-risk/map>. Accessed 4 May 2020.
- UNEP. (2009). *Rainwater harvesting: A lifeline for human well-being* (80 pp.). United Nations Environment Programme. Open File Rep.

- UNITAR (United Nation Institute for Training and Research). (2021). *Satellite detected water extent between 9 & 15 September 2020 in Sennar, White Nile, and Al Jazira States, Sudan*. <https://www.unitar.org/maps/map/3123>. Accessed 3 Jan 2021.
- United Nations Office for Disaster Risk Reduction (UNDRR). (2021). *About the Sendai Framework*. <https://www.unisdr.org>. Accessed 7 Jan 2021.
- Wheeler, K. G., Basheer, M., Mekonnen, Z. T., Eltoum, S. O., Mersha, A., Abdo, G. M., Zagona, E. A., Hall, J. W., & Dadson, S. J. (2016). Cooperative filling approaches for the Grand Ethiopian Renaissance Dam. *Water International*, 41(4), 611–634. <https://doi.org/10.1080/02508060.2016.1177698>
- Wolock, D. M., & McCabe, G. J. (1995). Comparison of single and multiple flow direction algorithms for computing topographic parameters in TOPMODEL. *Water Resources Research*, 31(5), 1315–1324.
- Wright, R. (2014). *What goes into a flood map: Infographic*. <https://www.fema.gov/> Accessed 9 Sept 2020.
- Yagoub, M. M., Aishah, A., Elfadil, A. M., Periyasamy, P., Reem, A., Salama, A., & Yaqein, A. (2020). Newspapers as a validation proxy for GIS modeling in Fujairah, United Arab Emirates: Identifying flood-prone areas. *Natural Hazards*, 104(1), 111–141. <https://doi.org/10.1007/s11069-020-04161-y>
- Yang, K., Chen, F., He, C., Zhang, Z., & Long, A. (2020). Fuzzy risk analysis of dam overtopping from snowmelt floods in the nonstationarity case of the Manas River catchment, China. *Natural Hazards*. <https://doi.org/10.1007/s11069-020-04143-0>